

# EFFECT OF AN ADDITIONAL SENSOR ON AOA LOCALIZATION PERFORMANCE

Kutluyil Doğançay

School of Electrical and Information Engineering, University of South Australia  
Mawson Lakes, SA 5095, Australia  
Email: kutluyil.dogancay@unisa.edu.au

## ABSTRACT

This paper investigates the contribution of an additional sensor to the performance of a passive AOA emitter localization system. This problem arises in localization applications where additional sensor resources become available and there is a need to determine where the new sensor should be placed in order to achieve maximum performance improvement. The paper considers optimal placement of an additional sensor and shows that optimal sensor placement is determined by its angular position rather than the emitter range. The results of the paper are illustrated with simulation studies.

## 1. INTRODUCTION

The objective of passive emitter localization is to determine the location of an emitter by processing the emitter signals received by several sensors or a moving sensor platform. Passive emitter localization finds application in mobile communications, wireless sensor networks and electronic warfare, to name but a few. The receiving platforms may employ sensors capable of measuring angle of arrival (AOA), time of arrival (TOA), time difference of arrival (TDOA), scan time, Doppler shift or received signal strength. Hybrid localization techniques combining some of these measurements are also available.

In this paper we consider optimal sensor placement for AOA localization employing stationary receiving platforms. The AOA localization problem has a rich history (see e.g. [1]). The key idea is to triangulate multiple bearing lines emanating from sensors. The approach adopted in this paper is to find optimal sensor locations by maximizing the determinant of the Fisher information matrix [2]. This is equivalent to minimizing the estimation uncertainty. The Fisher information matrix may be approximated by replacing the true emitter location with its maximum likelihood estimate [3]. Optimal sensor placement methods for AOA localization have been developed in [4]. The particular problem that is of interest to us in this paper is the quantification of performance improvement to be had by allocating an additional AOA sensor to an existing AOA localization system. This then naturally leads to another optimization problem which has the objective of finding the optimal placement for the additional sensor based on the knowledge of other sensors' positions and a rough idea of the emitter location. An elegant closed-form solution to this optimization problem is developed. The simplicity of the optimal solution makes it well-suited for practical implementation in sensor allocation problems with redeployable sensors.

The paper is organized as follows. Section 2 provides an outline of the AOA localization problem and derives the Fisher information matrix for AOA localization. Section 3

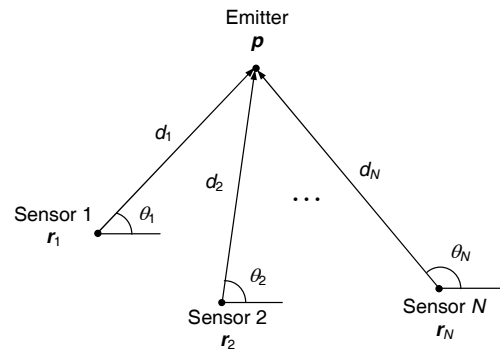


Figure 1: Two-dimensional AOA emitter localization.

derives a useful alternative expression for the Fisher information matrix (FIM) that facilitates further analysis. The effect of an additional AOA sensor on FIM is discussed in Section 4. The optimum placement for the new sensor is also analyzed and a new elegant solution is derived. Section 5 presents simulation studies to demonstrate the results of the paper. Conclusions are drawn in Section 6.

## 2. AOA LOCALIZATION

We consider 2D localization by AOA measurements taken at multiple sensors. The general AOA localization problem employing  $N$  sensors is depicted in Fig. 1 where  $p = [p_x, p_y]^T$  is the unknown emitter location with  $T$  denoting matrix transpose and  $r_i = [x_i, y_i]^T$  is the location of the  $i$ th sensor,  $1 \leq i \leq N$ . The objective of AOA emitter localization is to estimate the emitter location  $p$  from a set of bearing measurements collected by  $N$  sensors. The estimation process involved triangulation of the bearing lines emanating from the sensors. The minimum number of AOA sensors required for 2D emitter localization is two. However the larger  $N$  the better the localization performance will be. The AOA measurement at sensor  $i$  is given by

$$\tilde{\theta}_i = \theta_i + n_i, \quad \theta_i = \tan^{-1} \frac{p_y - y_i}{p_x - x_i} \quad (1)$$

where  $n_i \sim \mathcal{N}(0, \sigma^2)$  is the additive i.i.d. zero-mean Gaussian noise with variance  $\sigma^2$ . For simplicity all sensors are assumed to have identical noise variance regardless of the emitter range.

The Fisher information matrix (FIM) for AOA localization is [5]

$$\Phi = \begin{bmatrix} \phi_{11} & \phi_{12} \\ \phi_{21} & \phi_{22} \end{bmatrix} = J_o^T \Sigma^{-1} J_o \quad (2)$$

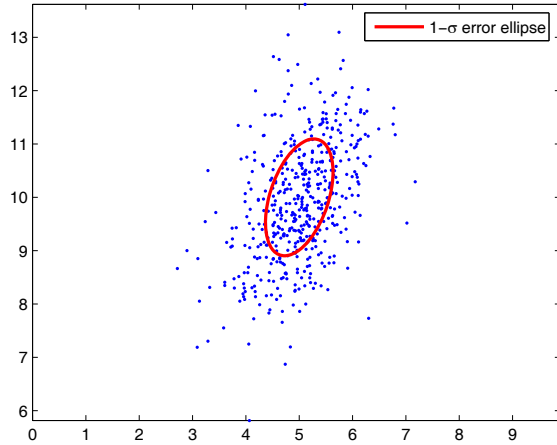


Figure 2: Illustration of  $1\text{-}\sigma$  error ellipse and a realization of estimates. The area of the ellipse is  $A_{1\sigma} = \pi/|\Phi|^{1/2}$ .

where  $J_o$  is the Jacobian evaluated at the true emitter location

$$J_o = \begin{bmatrix} u_1^T/d_1 \\ u_2^T/d_2 \\ \vdots \\ u_N^T/d_N \end{bmatrix}, \quad u_i = \begin{bmatrix} -\sin \theta_i \\ \cos \theta_i \end{bmatrix}, \quad d_i = \|p - r_i\| \quad (3)$$

and  $\Sigma$  is the AOA noise covariance matrix

$$\Sigma = \sigma^2 \begin{bmatrix} 1 & & & 0 \\ & \ddots & & \\ & & \ddots & \\ 0 & & & 1 \end{bmatrix}_{N \times N}. \quad (4)$$

FIM can be rewritten as

$$\Phi_N = \frac{1}{\sigma^2} \sum_{i=1}^N \frac{1}{d_i^2} u_i u_i^T. \quad (5)$$

Here

$$u_i = \begin{bmatrix} 0 & -1 \\ 1 & 0 \end{bmatrix} \frac{p - r_i}{d_i} \quad (6)$$

is a unit vector orthogonal to the bearing vector emanating from the  $i$ th sensor.

**Observation 1** *Moving a sensor from  $r_i$  to  $2p - r_i$  (i.e., reflecting the sensor about the emitter) does not affect FIM.*

This is easily seen from (5) where replacing  $u_i$  with  $-u_i$  for any  $i$ ,  $1 \leq i \leq N$ , does not change FIM. In (6) substituting  $2p - r_i$  for  $r_i$  results in  $u_i$  becoming  $-u_i$ , which verifies the observation [4]. This property allows us to generate new optimal geometries from a given optimal localization geometry by simply reflecting some of the sensors about the emitter location.

As illustrated in Fig. 2, the area of the  $1\text{-}\sigma$  error ellipse (39.4% uncertainty region) of an efficient estimator is given by  $A_{1\sigma} = \pi/|\Phi|^{1/2}$  where  $|\cdot|$  denotes determinant. In this paper we employ the criterion of maximizing the determinant

of FIM, which is equivalent to minimizing the area of uncertainty ellipse, for finding the optimal sensor locations [2]. This criterion tacitly assumes that the localization algorithm in use is nearly efficient so that its error covariance can be approximated by CRLB, which is the inverse of FIM. The equivalence of maximization of the determinant of FIM to minimization of MSE (the trace of CRLB) has been shown elsewhere [4].

### 3. ALTERNATIVE EXPRESSION FOR AOA FIM

In this section we will express FIM in an alternative way that lends itself into further scrutiny. Writing  $u_i = [u_x(i), u_y(i)]^T$  we have

$$u_i u_i^T = \begin{bmatrix} u_x^2(i) & u_x(i)u_y(i) \\ u_x(i)u_y(i) & u_y^2(i) \end{bmatrix} \quad (7)$$

and

$$\Phi_N = \frac{1}{\sigma^2} \begin{bmatrix} \sum_i \frac{1}{d_i^2} u_x^2(i) & \sum_i \frac{1}{d_i^2} u_x(i)u_y(i) \\ \sum_i \frac{1}{d_i^2} u_x(i)u_y(i) & \sum_i \frac{1}{d_i^2} u_y^2(i) \end{bmatrix} \quad (8a)$$

$$= \frac{1}{\sigma^2} \begin{bmatrix} \sum_i \frac{1}{d_i^2} \sin^2 \theta_i & -\sum_i \frac{1}{d_i^2} \sin \theta_i \cos \theta_i \\ -\sum_i \frac{1}{d_i^2} \sin \theta_i \cos \theta_i & \sum_i \frac{1}{d_i^2} \cos^2 \theta_i \end{bmatrix} \quad (8b)$$

$$= \frac{1}{\sigma^2} \begin{bmatrix} \frac{1}{2} \sum_i \frac{1}{d_i^2} (1 - \cos 2\theta_i) & -\frac{1}{2} \sum_i \frac{1}{d_i^2} \sin 2\theta_i \\ -\frac{1}{2} \sum_i \frac{1}{d_i^2} \sin 2\theta_i & \frac{1}{2} \sum_i \frac{1}{d_i^2} (1 + \cos 2\theta_i) \end{bmatrix}. \quad (8c)$$

The determinant of FIM can therefore be written as

$$|\Phi_N| = \frac{1}{4\sigma^4} \left( \left( \sum_{i=1}^N \frac{1}{d_i^2} \right)^2 - \left( \sum_{i=1}^N \frac{1}{d_i^2} \sin 2\theta_i \right)^2 - \left( \sum_{i=1}^N \frac{1}{d_i^2} \cos 2\theta_i \right)^2 \right). \quad (9)$$

Since  $|\Phi_N| \geq 0$ , for fixed  $d_i$  the maximization of  $|\Phi_N|$  over  $\theta_i$  is equivalent to the minimization of

$$\left( \sum_{i=1}^N \frac{1}{d_i^2} \sin 2\theta_i \right)^2 + \left( \sum_{i=1}^N \frac{1}{d_i^2} \cos 2\theta_i \right)^2 \quad (10)$$

over  $\theta_i$ .

### 4. EFFECT OF ADDITIONAL SENSOR

For a given AOA localization geometry with  $N$  sensors the determinant of Fisher information matrix (FIM) is given by (9). Suppose that another sensor is added to the system bringing the number of sensors to  $N + 1$ . The increase in the determinant of FIM due to the inclusion of the  $(N + 1)$ th sensor can be expressed as

$$|\Phi_{N+1}| - |\Phi_N| = \frac{1}{2\sigma^4 d_{N+1}^2} \left( \sum_{i=1}^N \frac{1}{d_i^2} - \sin 2\theta_{N+1} \sum_{i=1}^N \frac{1}{d_i^2} \sin 2\theta_i - \cos 2\theta_{N+1} \sum_{i=1}^N \frac{1}{d_i^2} \cos 2\theta_i \right). \quad (11)$$

Applying the trigonometric identity  $\cos(a - b) = \cos a \cos b + \sin a \sin b$  to the above expression, we obtain

$$|\Phi_{N+1}| - |\Phi_N| = \frac{1}{2\sigma^4 d_{N+1}^2} \sum_{i=1}^N \frac{1}{d_i^2} (1 - \cos 2(\theta_i - \theta_{N+1})). \quad (12)$$

An analysis of (12) leads to the conclusion that we have  $|\Phi_{N+1}| > |\Phi_N|$ , i.e., the additional sensor improves the localization performance, unless

- $d_{N+1} \rightarrow \infty$ , or
- $\theta_i = \theta_{N+1}$  for  $i = 1, \dots, N$ , implying all bearing vectors are aligned,

in which case  $|\Phi_{N+1}| = |\Phi_N|$ , i.e., the additional sensor does not improve the localization performance. In practice the first case arises if the new sensor is too far away from the emitter. The second case occurs when the range-to-baseline ratio is extremely large.

An increase in the determinant of FIM leads to a smaller uncertainty area (better estimation performance) since the area of the  $1-\sigma$  error ellipse (39.4% uncertainty region) is given by  $A_{1\sigma} = \pi/|\Phi|^{1/2}$ .

Equation (12) also provides insight into where the additional sensor should be placed to maximally improve the performance of an existing AOA localization system. Assuming that the range of the new sensor  $d_{M+1}$  is fixed, the optimal bearing angle  $\theta_{N+1}$  is obtained from

$$\theta_{N+1}^* = \arg \max_{\theta_{N+1}} \sum_{i=1}^N \frac{1}{d_i^2} (1 - \cos 2(\theta_i - \theta_{N+1})) \quad (13a)$$

$$= \arg \min_{\theta_{N+1}} \sum_{i=1}^N \frac{1}{d_i^2} \cos 2(\theta_i - \theta_{N+1}). \quad (13b)$$

Note that the optimal angle  $\theta_{N+1}^*$  is independent of the new sensor range  $d_{N+1}$ . Defining

$$v_i = \begin{bmatrix} \cos 2\theta_i \\ \sin 2\theta_i \end{bmatrix}, \quad s = \sum_{i=1}^N \frac{1}{d_i^2} v_i \quad (14)$$

(13b) can be equivalently written as

$$\theta_{N+1}^* = \begin{cases} -\frac{1}{2}(\pi - \angle s) \\ -\frac{1}{2}(\pi - \angle s) + \pi \end{cases} \quad (15)$$

where  $\angle s$  denotes the bearing angle of  $s$ . We formally have the following theorem:

**Theorem 1** *The optimum AOA angle for an additional  $(N + 1)$ th sensor maximizing the performance improvement of an AOA localization system is given by (15).*

This optimization problem can be interpreted as follows. Find the sum of vectors  $v_i$  weighted by  $1/d_i^2$ . Determine the rotation angle for the sum vector that makes it aligned with the negative  $x$ -axis. This solves the minimization problem in (13b). Half of the negative rotation angle gives the optimal bearing angle for the additional sensor. From Observation 1 we see that adding  $\pi$  rad to the optimal angle does not affect FIM, thereby giving another optimal angle.

## 5. SIMULATION STUDIES

Several AOA localization geometries have been simulated to demonstrate the application of Theorem 1. All simulated geometries have  $N = 4$  sensors with AOA noise variance  $5^\circ$ . The emitter is at the origin. In the first simulated geometry the emitter ranges are  $d_1 = 100$  km,  $d_2 = 90$  km,  $d_3 = 70$  km and  $d_4 = 80$  km. The AOA angles are  $\theta_1 = 0^\circ$ ,  $\theta_2 = 30^\circ$ ,  $\theta_3 = 50^\circ$  and  $\theta_4 = 80^\circ$ . A fifth AOA sensor is added to the system at range  $d_5 = 120$  km. Fig. 3 shows the variation of determinant of FIM as a function of  $\theta_5$  and the determinant of FIM for the original system with four sensors. The additional sensor is seen to increase the determinant of FIM as expected. The maximal increase is attained at  $\theta_5^*$  given by (15). Fig. 4 shows the original geometry and the geometry with the optimally placed additional sensor. The  $1-\sigma$  error ellipses and uncertainty areas are compared in Fig. 5. The top error ellipse is for the original geometry and the lower error ellipse is obtained after the addition of another sensor that is optimally positioned. The lower error ellipse has a smaller area, confirming the performance improvement achieved.

In the second simulation example the emitter ranges are set to  $d_1 = 60$  km,  $d_2 = 90$  km,  $d_3 = 60$  km and  $d_4 = 50$  km. The AOA angles are  $\theta_1 = 0^\circ$ ,  $\theta_2 = 90^\circ$ ,  $\theta_3 = -90^\circ$  and  $\theta_4 = 180^\circ$ . A fifth AOA sensor is added to the system at range  $d_5 = 80$  km. Fig. 6 shows the variation of determinant of FIM as a function of  $\theta_5$  and the determinant of FIM for the original system with four sensors. Fig. 7 shows the original geometry and the geometry with the optimally placed additional sensor. Note that the original geometry has almost optimal sensor placement. The optimal position for the additional sensor is aligned with one of the sensors having a large range. This is intuitively expected as it reduces the variance of the AOA measurement taken by the sensor at long range. The  $1-\sigma$  error ellipses and uncertainty areas are compared in Fig. 8.

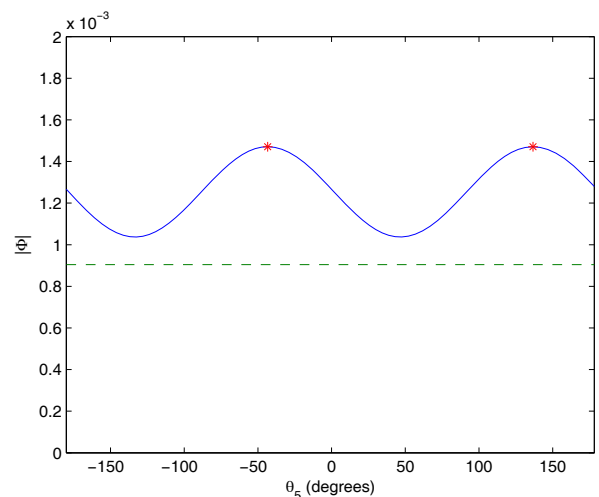


Figure 3: Determinant of FIM with additional sensor as a function of its AOA angle  $\theta_5$  and determinant of FIM for original system with four sensors (dashed line). Determinant of FIM is maximized at  $\theta_5^* = -43.3735^\circ$  and  $136.6265^\circ$  marked with “\*”.

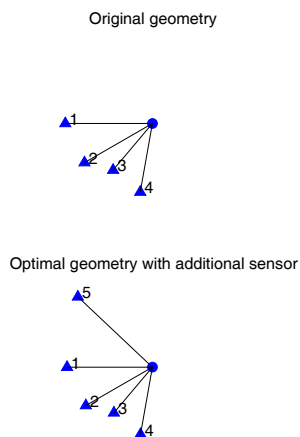


Figure 4: Original geometry and same geometry with optimally placed additional sensor.

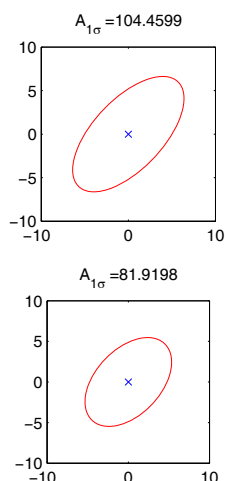


Figure 5: 1- $\sigma$  error ellipses for original geometry and after addition of an optimally placed sensor.

The emitter ranges are set to  $d_1 = 80$  km,  $d_2 = 90$  km,  $d_3 = 80$  km and  $d_4 = 100$  km in the final simulation example. The AOA angles are  $\theta_1 = 0^\circ$ ,  $\theta_2 = 10^\circ$ ,  $\theta_3 = -20^\circ$  and  $\theta_4 = 30^\circ$ . A fifth AOA sensor is added to the system at range  $d_5 = 80$  km. Fig. 9 shows the variation of determinant of FIM as a function of  $\theta_5$  and the determinant of FIM for the original system with four sensors. Fig. 10 shows the original geometry and the geometry with the optimally placed additional sensor. The optimal placement of the additional sensor resembles an almost perpendicular separation between the clustered original system sensors and the new sensor. The 1- $\sigma$  error ellipses shown in Fig. 11 indicate a significant performance improvement achieved by the optimally placed new sensor.

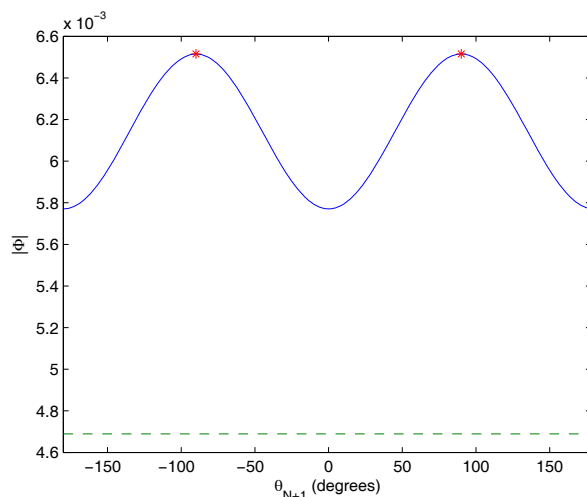


Figure 6: Determinant of FIM with additional sensor as a function of its AOA angle  $\theta_5$  and determinant of FIM for original system with four sensors (dashed line).

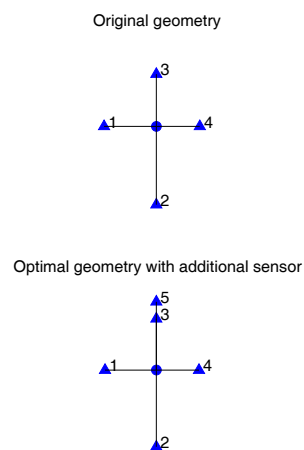


Figure 7: Original geometry and same geometry with optimally placed additional sensor.

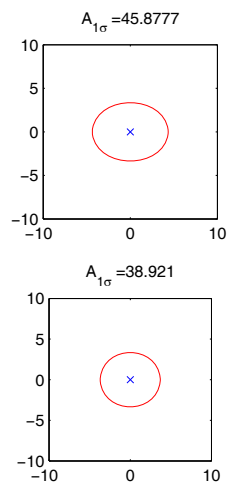


Figure 8: 1- $\sigma$  error ellipses for original geometry and after addition of an optimally placed sensor.

## 6. CONCLUSION

This paper has analyzed the performance improvement contributed by an additional AOA sensor to an existing AOA localization system. Optimal placement of the new sensor in order to maximize the performance improvement was also considered. The analysis led to the derivation of elegant optimization results for AOA sensor placement. The analysis assumed prior knowledge of the emitter location. This is not a major impediment to the usefulness of the results since a rough idea of the emitter location is often sufficient to obtain sensor placement results leading to significantly superior performance. The effectiveness of the results was illustrated with several simulation studies.

## REFERENCES

- [1] S. C. Nardone and M. L. Graham, "A closed-form solution to bearings-only target motion analysis," *IEEE Journal of Oceanic Eng.*, vol. 22, no. 1, pp. 168–178, January 1997.
- [2] Y. Oshman and P. Davidson, "Optimization of observer trajectories for bearings-only target localization," *IEEE Trans. on Aerospace and Electronic Systems*, vol. 35, no. 3, pp. 892–902, 1999.
- [3] K. Doğançay, "Online optimization of receiver trajectories for scan-based emitter localization," *IEEE Trans. on Aerospace and Electronic Systems*, vol. 43, no. 3, pp. 1117–1125, July 2007.
- [4] K. Doğançay and H. Hmam, "Optimal angular sensor separation for AOA localization," *Signal Processing*, vol. 88, no. 5, pp. 1248–1260, May 2008.
- [5] D. J. Torrieri, "Statistical theory of passive location systems," *IEEE Trans. on Aerospace and Electronic Systems*, vol. 20, pp. 183–198, March 1984.

Original geometry



Optimal geometry with additional sensor

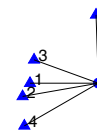


Figure 10: Original geometry and same geometry with optimally placed additional sensor.

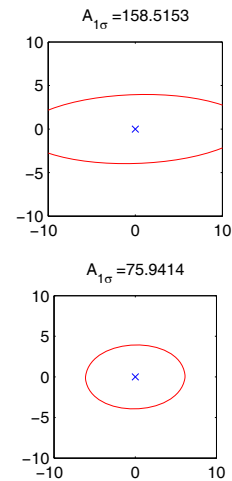


Figure 11: 1- $\sigma$  error ellipses for original geometry and after addition of an optimally placed sensor.

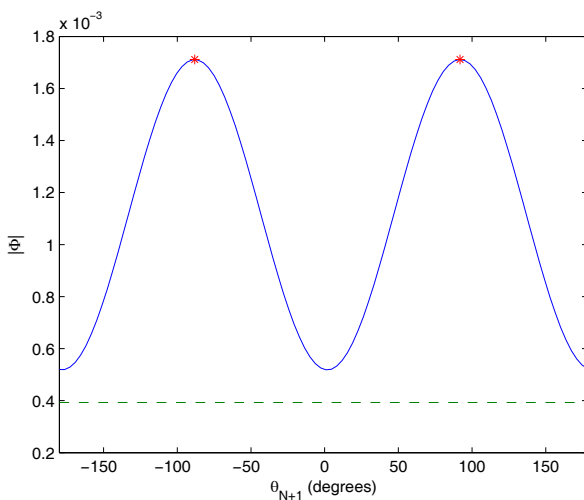


Figure 9: Determinant of FIM with additional sensor as a function of its AOA angle  $\theta_5$  and determinant of FIM for original system with four sensors (dashed line).